



# Effect of light intensity on the accumulation of protostane triterpenes in Asian water plantain (*Alisma orientale*)

Wenqing Wu<sup>1</sup> · Simeng Li<sup>1</sup> · Wei Gu<sup>1,2</sup> · Rong Tian<sup>1</sup> · Man Luo<sup>1</sup> · Junjie Tang<sup>1</sup> · Min Tang<sup>1</sup> · Yinzhi Wu<sup>1</sup>

Received: 31 July 2023 / Revised: 27 December 2023 / Accepted: 8 February 2024 / Published online: 27 February 2024  
© The Author(s) under exclusive licence to Franciszek Górski Institute of Plant Physiology, Polish Academy of Sciences, Kraków 2024

## Abstract

*Alismatis rhizoma* is an essential medicine in clinical practice. Asian water plantain (*Alisma orientale* (Sam.) Juzep) is one of the original plants of *Alismatis rhizoma*. Previous studies have identified the optimal light intensity range for the growth and development of *A. orientale*, but the mechanism by which light intensity affects the accumulation of secondary metabolites of *A. orientale* is unknown. The aim of this study was to investigate the effect of light intensity on the accumulation of triterpenoids in *A. orientale* saplings and its potential molecular mechanism. The dry weight and contents of total triterpenes and indicative components (alisol B 23-acetate and alisol C 23-acetate) as well as the expression of key enzyme genes in the triterpene biosynthesis pathway under different light intensities (50–600  $\mu\text{mol m}^{-2}\cdot\text{s}^{-1}$ ) were determined. The results showed that the accumulation of dry matter and the contents of total triterpenes, alisol B 23-acetate, and alisol C 23-acetate increase first and then decrease with increasing light intensity, with the maximum values of 31.65 g, 18.35  $\text{mg}\cdot\text{g}^{-1}$ , 1.91  $\text{mg}\cdot\text{g}^{-1}$ , and 0.13  $\text{mg}\cdot\text{g}^{-1}$  recorded at light intensities of 400, 200, and both of 300  $\mu\text{mol m}^{-2}\cdot\text{s}^{-1}$ , respectively. Light intensities of 200–400  $\mu\text{mol m}^{-2}\cdot\text{s}^{-1}$  promote the expressions of key enzyme genes and the accumulation of total triterpenes significantly. Correlation analysis showed that the expression levels of key enzyme genes are significantly correlated with total triterpene and indicative component contents, and these correlations are strongest under moderate light intensities. Overall, our results reveal that a moderate light intensity of 200–400  $\mu\text{mol m}^{-2}\cdot\text{s}^{-1}$  is beneficial for the growth and synthesis of protostane triterpenes in *A. orientale* seedlings, and that its probable mechanism involves the upregulated expression of enzymes that are key in the synthesis of triterpenoid ingredients. This study clarified the suitable light intensity range for the synthesis and accumulation of protostane triterpenes of *A. orientale*, which provided scientific basis for the production of high-quality superior forms of *A. orientale*.

**Keywords** *Alisma orientale* (Sam.) Juzep · Asian water plantain · Light intensity · Protostane triterpenes · Gene expression

## Introduction

*Alisma orientale* (Sam.) Juzep. is a perennial herb of the genus *Alismataceae* that is widely cultivated in the Fujian, Jiangxi, Sichuan, and Jilin provinces of China. Particularly

large amounts are produced in Fujian Province and used to produce ‘Jianzexie’, a medicinal preparation known for its high quality and clinical efficacy.

The dried tubers of *A. orientale* are termed ‘*Alismatis rhizome*’ and widely used in traditional Chinese medicine for its dampness-removing, water-promoting, heat-relieving, turbidification, and lipid-lowering effects. Accordingly, it is a well-regarded traditional remedy for nephritic edema, pyelonephritis, enteritis, and diarrhea, among other conditions (Shu et al. 2016). Triterpenoids are the active components through which *Alismatis rhizoma* exerts its pharmacological effects (Choi et al. 2019; Gao et al. 2018). At present, more than 110 kinds of triterpenoids have been isolated from *Alismatis rhizoma*, most being protostane triterpenes (Wang et al. 2020a; Zhang et al. 2017a). Protostanes have a narrow natural distribution and are unique to few plant groups.

Communicated by V.P. Singh.

Wenqing Wu and Simeng Li contributed equally to this work.

✉ Wei Gu  
guwei2288@126.com

<sup>1</sup> School of Pharmacy, Nanjing University of Chinese Medicine, Nanjing 210023, China

<sup>2</sup> Jiangsu Collaborative Innovation Center of Chinese Medicinal Resources Industrialization, Nanjing University of Chinese Medicine, Nanjing 210023, China

Accordingly, they are considered to be chemical classification markers of the genus *Alismataceae* (Jang and Lee 2021). The triterpenes alisol B 23-acetate ( $C_{32}H_{50}O_5$ ) and alisol C 23-acetate ( $C_{32}H_{48}O_6$ ) show a variety of biological activities and is the main material basis of pharmacological effects of *Alismatis rhizoma*, including liver-protection, diuresis, anti-stone, kidney protection, anti-inflammation, blood lipid lowering, liver protection, blood glucose lowering, and anti-cancer. (Cheng and Ouyang 2023; Fan et al. 2021; Hwang et al. 2016; Shen et al. 2020; Wu et al. 2023; Zhu et al. 2021; Feng et al. 2021). It has good clinical efficacy in the treatment of kidney stones, inflammation, tumor, cardiovascular disease, anti-atherosclerosis, cancer and osteoporosis. (Dou, et al. 2018; Jang and Lee 2021; Luan et al. 2021; Xu et al. 2020; Yan et al. 2022; Zhang et al. 2017b; Zhou et al. 2023).

The main synthetic pathway for triterpenes in plants is the mevalonate pathway, in which acetyl-CoA acts as the substrate to synthesize intermediate isopentenyl pyrophosphates (IPPs) catalyzed by the key enzymes 3-hydroxy-3-methylglutaryl-CoA reductase (HMGR) and mevalonate pyrophosphate decarboxylase (MVD). Subsequently, IPPs form triterpenoid skeletons under the action of farnesyl pyrophosphate synthase (FPPS), squalene synthetase (SS), squalene epoxidase (SE) (Yao et al. 2020), as shown in Fig. 1.

The quality of traditional Chinese medicine is evaluated by reference to a comprehensive index termed ‘the

authenticity of medicinal materials.’ Plant characteristics related to this index are largely dictated its environment and germplasm. The growth and development of medicinal plants and the accumulation of medicinal components are closely related to various environmental factors (Li et al. 2020). As photoautotrophs, medicinal plants are affected by light-environment factors (light intensity, light quality, photoperiod, and light direction) during their entire growth and development (Roeber et al. 2021). Photosynthesis is the process by which plants produce their own assimilates and a high-energy reaction related to the intensity of light energy. As a key way for plants to obtain energy, photosynthesis provides ATP molecules (energy) and NADPH molecules (electron) for carbon fixation. The resulting photosynthates provide carbon sources for primary metabolism, and the primary metabolic derivatives provide small-molecule precursor substrates for secondary metabolism. Light intensity is one of the key factors affecting plant photosynthesis, externally affecting their growth, development, and appearance, and internally affecting their physiological, biochemical, and metabolic processes (Huang et al. 2022). Light intensity can affect the size, color, and morphology of plant stems and leaves, as well as plant photosynthesis, thus affecting the yield and quality of medicinal plant tissues and organs (Zheng et al. 2017). Light intensity affects the primary metabolic processes of plants by regulating their photosynthetic

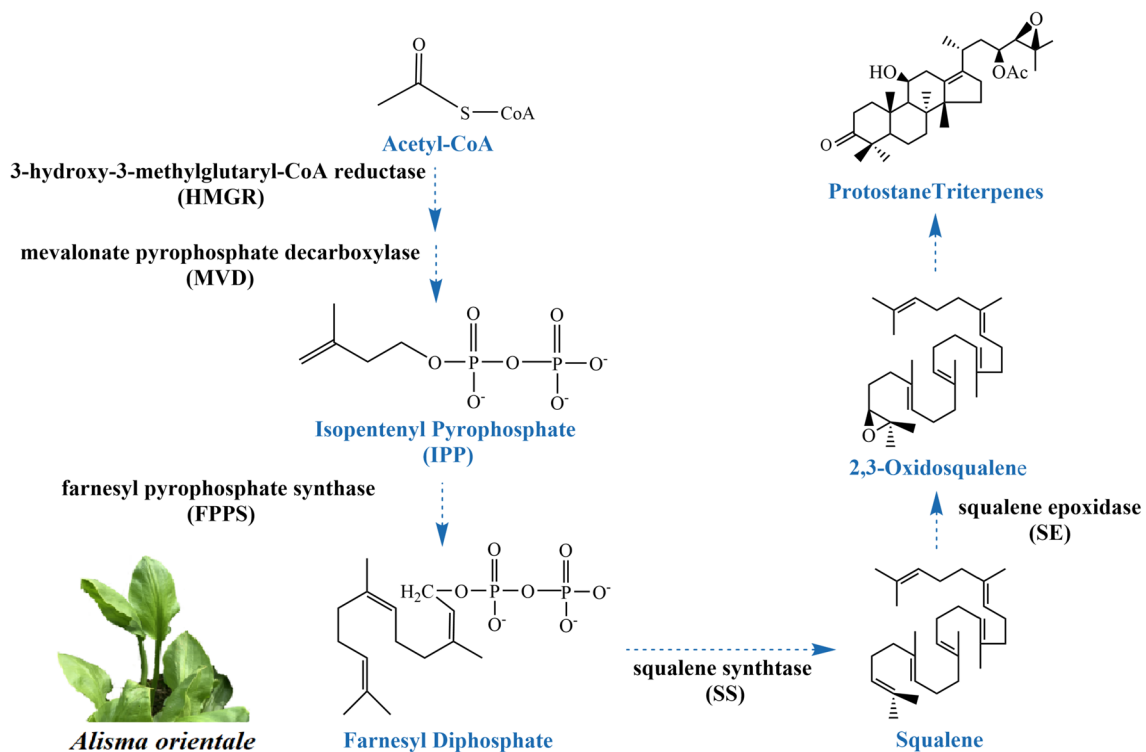


**Fig. 1** The schematic diagram of triterpene biosynthesis pathway

rates, affecting the accumulation of secondary metabolites (Kuo et al. 2020). Previous study determined that the suitable light intensity range for the growth of *A. orientale* was 200–400  $\mu\text{mol m}^{-2}\cdot\text{s}^{-1}$ . Under this light intensity range, *A. orientale* has good apparent morphology, strong growth, good photosynthetic characteristics and strong antioxidant capacity (Ji et al. 2023). For triterpenoid secondary metabolites, the substrates are derived from the glycolytic metabolite pyruvate, deoxyxylose 5-phosphate, which is derived from the MEP pathway in the plastids, and pyruvate derivative acetyl-CoA, which is derived from mevalonate, which is derived from the cytoplasmic MVA pathway. However, the mechanism by which light intensity affects the growth and accumulation of secondary metabolites in *A. orientale* is still unclear. Accordingly, in the present study, we investigated the effect of light intensity on the accumulation of active components in *A. orientale* and its molecular mechanism by analyzing the dry matter accumulation, total triterpenes, index components, and expression of key enzymes in the triterpene biosynthesis pathway of *A. orientale* seedlings reared under different lighting conditions. Consequently, we identify the most suitable light-intensity range for the synthesis and accumulation of protostane triterpenes in *A. orientale* and provide a scientific basis for its high-quality and efficient production.

## Materials and methods

### Plant materials

Plant materials were collected from Jianou, Fujian Province and identified as *A. orientale* by Professor Gu Wei (College of Pharmacy, Nanjing University of Chinese Medicine). In early August, pest- and disease-free *A. orientale* seedlings with strong and consistent growth were transferred to the artificial climate chamber of Nanjing University of Chinese Medicine for light treatment, and the light intensity was controlled by a lift-off LED lamp. Five levels of light intensity were chosen based on the natural light intensity of Jian'ou City, Fujian Province during the growing period of *A. orientale* provided by the China Meteorological Data Center. The average light intensity for each treatment group was determined using a photosynthetic apparatus (LI-6400XT, LI-COR company, USA) as follows: G1 (50  $\mu\text{mol m}^{-2}\cdot\text{s}^{-1}$ ), G2 (100  $\mu\text{mol m}^{-2}\cdot\text{s}^{-1}$ ), G3 (200  $\mu\text{mol m}^{-2}\cdot\text{s}^{-1}$ ), G4 (300  $\mu\text{mol m}^{-2}\cdot\text{s}^{-1}$ ), G5 (400  $\mu\text{mol m}^{-2}\cdot\text{s}^{-1}$ ), G6 (500  $\mu\text{mol m}^{-2}\cdot\text{s}^{-1}$ ), G7 (600  $\mu\text{mol m}^{-2}\cdot\text{s}^{-1}$ ). The seedlings were reared with under a 12 h  $\text{day}^{-1}$  light cycle at 60% humidity and 25 °C with regular watering. After 32 days of light treatment, the plants were harvested, washed quickly with water, sanitized in an oven at 105 °C for 15 min, and dried at 60 °C.

### Reagents

For determination of total triterpene content: Absolute ethanol (10,009,261, Sinopharm, China); 95% ethanol (100,091,643, Sinopharm, China); vanillin (H107521, Aladdin, Shanghai, China); acetic acid (200-580-7, Enox, Jiangsu, China); perchloric acid (P112070, Aladdin, Shanghai, China).

For determination of indicative components content: acetonitrile (HPLC-grade, TEDIA, USA); methanol (HPLC-grade, TEDIA, USA); H<sub>2</sub>O (Wahaha, China); alisol B 23-acetate standard (purity > 98%, B21641-20 mg, Yuanye Biotechnology, Shanghai, China); alisol C 23-acetate standard (purity > 98%, B21764-20 mg, Yuanye Biotechnology, Shanghai, China).

For analysis of key enzyme genes: RNAsimple Total RNA Kit (Cat. No. DP419; Tiangen, China); M-MLV reverse transcriptase (Cat. C28025021, Invitrogen, USA); Perfectstart® Green qPCR SuperMix (AQ610, TransGen Biotech, Beijing, China).

### Dry-weight measurement

The weights of the dried roots, stems, and leaves of *A. orientale* were recorded, and the samples were crushed and passed through a No.5 sieve for further use.

### Determination of total triterpene content

Rhizome, tuber, and leaf samples (1.00 g) were accurately weighed into 100 mL glass-stoppered conical flasks, which were accurately weighed and heated at 57 °C in 25 mL of 70% ethanol for 46 min in a constant temperature water bath, then sonicated for 30 min (500 W, 40 kHz). After cooling to room temperature, 70% ethanol was added to regain the initial flask weight, and the extract was passed through a 0.22- $\mu\text{m}$  membrane filter.

Alisol B 23-acetate reference (2.0 mg) was accurately weighed into a 10-mL glass-stoppered conical flask and dissolved in absolute ethanol to obtain a standard solution with a concentration of 0.2  $\text{mg}\cdot\text{mL}^{-1}$ .

Total triterpenes were then determined by colorimetry with reference to a standard curve. To prepare the standard curve, aliquots of the standard solution (0.1, 0.2, 0.4, 0.6, 0.8, and 1.0 mL) were precisely pipetted to 10-mL glass-stoppered conical flasks and the solvent evaporated at 60 °C.

To each flask was added 0.2 mL of freshly prepared 5% vanillin/glacial acetic acid solution and 0.8 mL of perchloric acid. The solutions were mixed well, sealed, and heated at 60 °C for 15 min before being cooled in an ice bath for

5 min. Then, 4 mL glacial acetic acid was added. A reference solution that contained no analyte was also prepared.

The UV–Vis spectra of the standards were then recorded over the wavelength range 410–800 nm using the blank sample as a reference, and the maximum absorbance (555 nm) was recorded. A standard curve with absorbance ( $y$ ) as the vertical coordinate and concentration ( $x$ ) as the horizontal coordinate was prepared and subjected to regression analysis, yielding a linear correlation ( $R^2 = 0.9991$ ) represented by the equation  $y = 4.2775x + 0.0307$ .

The sample solutions (0.2 mL) were then subjected to UV–Vis analysis following the same procedure. The total triterpene content was calculated from the absorbance at 555 nm using the standard curve equation.

Finely powdered *A. orientale* (~0.5 g) was accurately weighed into a 50 mL glass-stoppered conical flask and precisely 25 mL of 70% acetonitrile was added. The filled flask was weighed to a precision of  $\pm 0.01$  g and then sonicated for 30 min (500 W, 40 kHz). After cooling to room temperature, more acetonitrile was added to regain the initial weight of the flask. The sample solution was then filtered through a 0.45- $\mu\text{m}$  membrane and analyzed by HPLC.

Standard solutions of alisol B 23-acetate and alisol C 23-acetate were prepared in acetonitrile to concentrations of 70 and 10  $\mu\text{g}\cdot\text{mL}^{-1}$ , respectively. The standard solutions were stored at 4 °C for later use.

Samples were analyzed using a Waters e2695 series HPLC system (Waters Corporation, Milford, MA, USA) equipped with a quaternary pump and a variable wavelength ultraviolet (UV) detector. Samples (20  $\mu\text{L}$ ) were applied to a C18 analytical column (5  $\mu\text{m}$ , 4.6  $\times$  250 mm; Diamonsil, Beijing, China) at a flow rate of 0.8  $\text{mL}\cdot\text{min}^{-1}$ . The mobile phase was 60% acetonitrile/water. The column temperature was maintained at 30 °C, and the detection wavelength was set at 208 nm for alisol B 23-acetate and 246 nm for alisol C 23-acetate.

The mixed reference solution obtained was diluted to different concentrations (alisol B 23-acetate concentrations: 26.25, 35.00, 43.75, 52.50, 61.25, 70.00  $\mu\text{g}\cdot\text{mL}^{-1}$ ; alisol C 23-acetate concentrations: 1.50, 2.50, 3.75, 5.00, 6.25, 7.50, 8.75, 10.00  $\mu\text{g}\cdot\text{mL}^{-1}$ ) and analyzed using the chromatographic conditions outlined above. A standard curve was drawn with concentration as the horizontal coordinate ( $x$ ,  $\mu\text{g}\cdot\text{mL}^{-1}$ ) and peak area ( $y$ ) as the vertical coordinate. The concentration range of alisol B 23-acetate was 26.25–70  $\mu\text{g}\cdot\text{mL}^{-1}$  and showed a good linear relationship with peak area. The linear regression equation for the standard curve was  $y = 30,188x - 269,962$  ( $R^2 = 0.999$ ). A similar process was used for alisol C 23-acetate, and the standard curve showed good linearity ( $y = 37632x + 219.1$ ;  $R^2 = 0.9994$ ) in the concentration range 1.5–10  $\mu\text{g}\cdot\text{mL}^{-1}$ . The concentrations of alisol B 23-acetate and alisol C

23-acetate in the samples were determined from their HPLC peak areas using the standard curve.

## Method validation

The method precision was validated by analyzing the mixed reference solution six times. The relative standard deviations (RSDs) for the peak areas of alisol B 23-acetate and alisol C 23-acetate were 1.54% and 2.06%, respectively.

Sample stability was verified by analyzing the same sample solution at 0, 2, 4, 8, 12, and 24 h after preparation. The RSDs of the peak areas were 1.86 and 1.42% for alisol B 23-acetate and alisol C 23-acetate, demonstrating that the samples were stable for 24 h.

The method reproducibility was verified by analyzing six different samples from the same group. The RSDs of the peak areas were 1.09 and 1.26% for alisol B 23-acetate and alisol C 23-acetate, respectively.

The average recovery of 23-acetylalisol B and Alisol C 23-acetate was 99.13 and 99.30%, and the RSD was 1.87 and 1.12%.

The test solution was determined according to the chromatographic conditions outlined above. The contents of 23-acetyl-alismatol B and 23-acetyl-alismatol C were calculated per gram of alismatol using the regression equation obtained from analysis of the reference solutions.

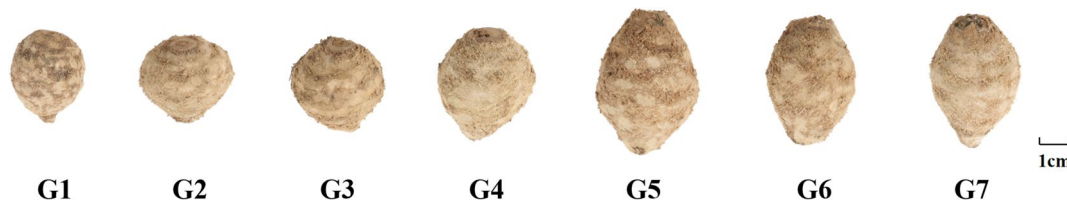
## Real-time fluorescence quantitative PCR

Total RNA was isolated using a simple total RNA kit. Products were subjected to electrophoresis on 1.0% agarose gels and quantified by electronic digital imaging using a Multi-Image light unit with the Alphamager HP platform. RNA purity and concentration were determined using Eppendorf UveVis spectrophotometers. cDNA was synthesized by reverse transcription of 1  $\mu\text{g}$  of total RNA using a reverse transcription kit and stored at  $-20$  °C.

Primer sequences for each gene were designed using Primer Premier 5.0 software, as shown in Table 1, and the primers were synthesized by Sangon Bioengineering (Shanghai, China), LTD. The PCR reaction system was operated as follows: the cells were treated with 2  $\mu\text{L}$  cDNA, 0.4  $\mu\text{L}$  Forward Primer, 0.4  $\mu\text{L}$  Reverse Primer, 10  $\mu\text{L}$  2  $\times$  Super Mix, 0.4  $\mu\text{L}$  Passive Reference Dye (50x), and 6.8  $\mu\text{L}$  dd  $\text{H}_2\text{O}$ . The reaction program was as follows: predeformation at 94 °C for 30 s, followed by 45 cycles of denaturation at 94 °C for 5 s, annealing at 60 °C for 34 s, and extension at 72 °C for 10 s. The relative expressions of genes for the five key enzymes were calculated using the  $2^{-\Delta\Delta\text{Ct}}$  method using the UBC gene as the reference gene.

**Table 1** Gst of primers used for qRT-PCR amplification

Gene	Forward Primer (5'-3')	Reverse Primer (5'-3')
UBC	TATGCTGGTGGGGTTTTTC	ATGCTCCCGTTACTATTGA
HMGR	GCTGCGGTGAATTGGATTG	GGGCAGACCAACAAGGTT
MVD	ATCAGCGTCACCCTCAACC	ACCCCTTTCTCCTCGTCTT
FPPS	CAACCTTAGGAATTCTGAACCAACA	AAAGGAGCTCAGTGAGGAGGAA
SS	TTTTACGCCTCTGGGTC	TTGGCACTTCATTTATGTCTT
SE	CCTTGATTGATGATAATGGGACT	GATGTCTACCTTTGCGGAGC

**Fig. 2** Tubers of *A. orientale* under different light intensities. G1 ( $50 \mu\text{mol m}^{-2}\cdot\text{s}^{-1}$ ), G2 ( $100 \mu\text{mol m}^{-2}\cdot\text{s}^{-1}$ ), G3 ( $200 \mu\text{mol m}^{-2}\cdot\text{s}^{-1}$ ), G4 ( $300 \mu\text{mol m}^{-2}\cdot\text{s}^{-1}$ ), G5 ( $400 \mu\text{mol m}^{-2}\cdot\text{s}^{-1}$ ), G6 ( $500 \mu\text{mol m}^{-2}\cdot\text{s}^{-1}$ ), G7 ( $600 \mu\text{mol m}^{-2}\cdot\text{s}^{-1}$ )

## Data processing and analysis

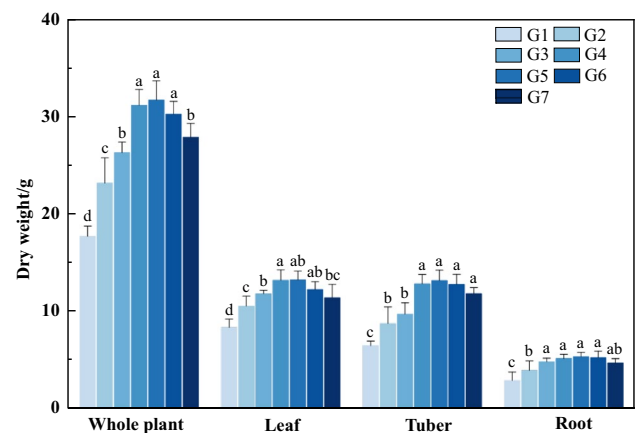
Significant differences between the interactions of varying key enzyme genes and effective components were determined using one-way and two-way analyses of variance. Significance levels were set at  $p \leq 0.05$ ,  $p \leq 0.01$ , indicated by \* and \*\*, respectively. Statistical analyses and graphic were generated in SPSS and Origin software.

## Results

### Dry matter accumulation and distribution

As shown in Fig. 2, the tuber volume of *A. orientale* showed obvious differences among the treatment groups. With the increase of light intensity, tuber volume first increased and then decreased. Transverse growth of *A. orientale* tubers was mainly observed in the G1–G2 groups, but their longitudinal growth was not significant. The tubers of the G3–G5 groups grew completely in both transverse and longitudinal directions, the maximum volume was observed for the G5 group (maximum tuber diameter 30.96 mm; height 58.54 mm). Compared with G3–G5, the tuber volumes for G6 and G7 were decreased but significantly larger than those for G1 and G2.

Light intensity affected dry matter accumulation of *A. orientale*, with significant differences observed for different light intensities. As shown in Fig. 3, with increasing of light intensity, the accumulation of dry matter in the leaves, tubers, roots, and whole plants all first increased and then decreased, reaching their maxima under G5 light

**Fig. 3** Dry weight of each part of *A. orientale* under different light intensities. The error bars represent the standard deviation. Different lowercase letters indicate significant differences ( $p \leq 0.05$ )

intensity, which were 31.65 g/plant, 13.20 g/plant, 13.15 g/plant and 5.30 g/plant. The dry weights of each part and the whole in the G1 group were the lowest at 17.64 g/plant, 8.32 g/plant, 6.44 g/plant and 2.89 g/plant. Compared with the minimum dry weight in group G1, the maximum dry weight of each part and whole plant in group G5 was increased by 79.4, 58.7, 104.2, and 83.4%.

These results indicate that increasing light intensity within a certain range is beneficial to dry matter accumulation in all plant parts and the whole plant, especially in the tubers. However, when light intensity exceeded a suitable light limit, dry matter accumulation was negatively affected, disrupting the normal growth of *A. orientale* seedlings.



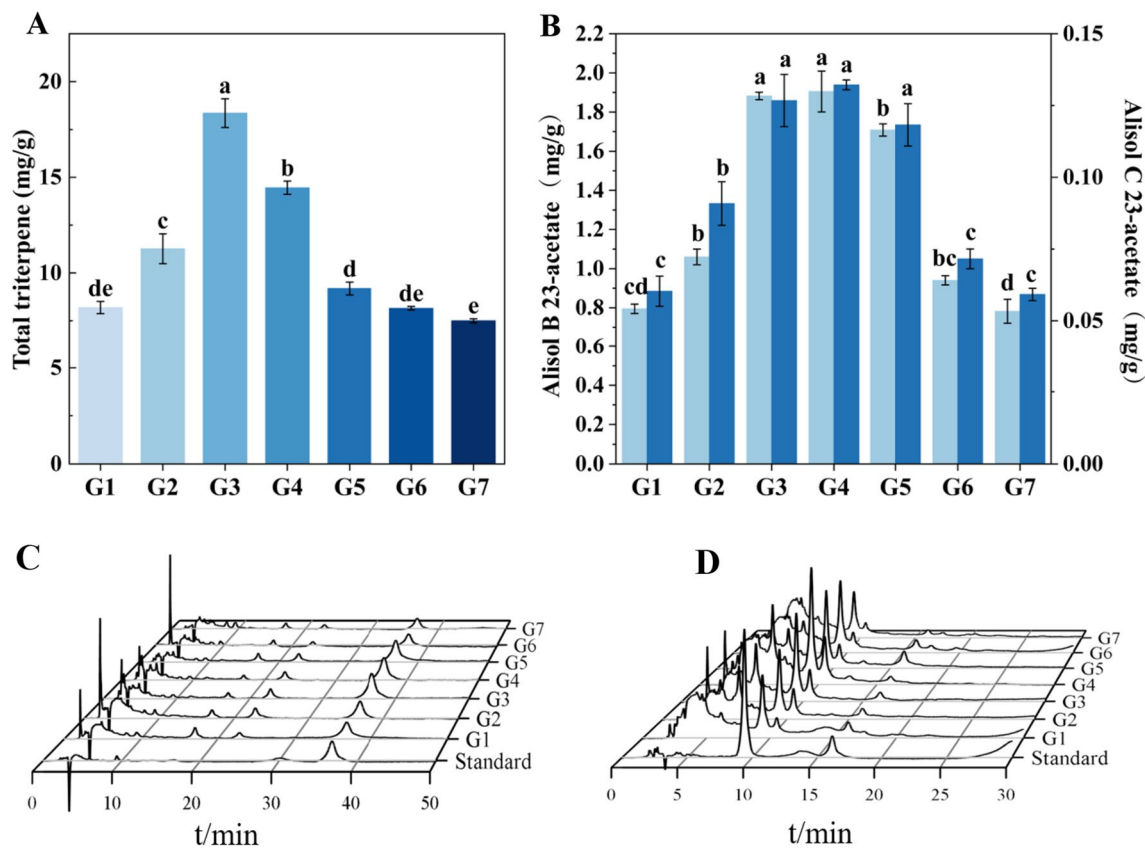


**Fig. 4** Content of effective components in *A. orientale* tuber under different light intensities. **A** Contents of total triterpenoid. **B** Contents of Alisol B 23-acetate and Alisol C 23-acetate. **C** HPLC chromatograms of Alisol B 23-acetate (208 nm). **D** HPLC chromatograms of

Alisol C 23-acetate (246 nm). The error bars represent the standard deviation. Different lowercase letters indicate significant differences ( $p \leq 0.05$ )

### Contents of total triterpenes and index components

The total triterpene contents of the *A. orientale* tubers were determined by UV spectrophotometry, and the results are shown in Fig. 4A. The content of total triterpenoids increased first and then decreased with increasing light intensity. The total triterpene content for the G3 group was significantly higher than that in the other groups ( $18.35 \text{ mg}\cdot\text{g}^{-1}$ ), which constitutes relative increases of 123.91% (G1), 62.89% (G2), 26.97% (G4), 99.69% (G5), 124.99% (G6), and 144.56% (G7). There were no significant differences among the G1, G6, and G7 groups.

The contents of alisol B 23-acetate and alisol C 23-acetate in the tubers of *A. orientale* reared under different light intensities were determined by HPLC. The content differences are shown in Fig. 4B, and the chromatographic graphs are shown in Fig. 4C and D. The results show that the contents of the two components in tubers increased first and then decreased with increasing light intensity. In general, the light intensity in the G3–G5 groups was

beneficial to the accumulation of alisol B 23-acetate and alisol C 23-acetate, with the highest values observed for G4 ( $1.91 \text{ mg}\cdot\text{g}^{-1}$  and  $0.13 \text{ mg}\cdot\text{g}^{-1}$ , respectively). The contents of alisol B 23-acetate were significantly different from those in the other groups except the G3 group, but the contents of alisol C 23-acetate were not significantly different from those in the G3 and G5 groups.

### Expression of key enzyme genes

As shown in Fig. 5, the expressions of the five key enzyme genes at different sites showed markedly different degrees of response to light intensity. In the leaves, the expression of the five key enzyme genes in G7 group was the lowest, and the key enzyme genes for HMGR, MVD, and SE in the G3 group were the highest, being 46.18-, 3.85-, and 168.65-times those for the G7 group. The expressions of FPPS and SS in the G4 group were the highest, being 30.35- and 30.13-times higher than those of the G7 group.

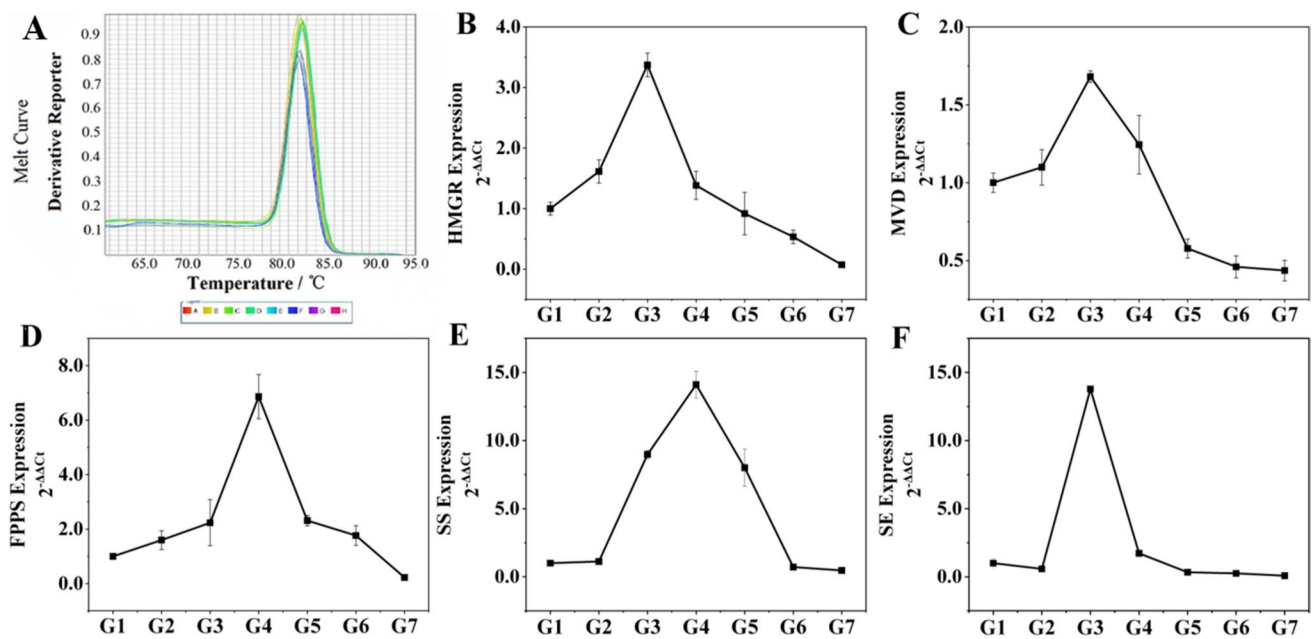


**Fig. 5** qRT-PCR melting curve and relative gene expression level under different light intensities. **A** Melt curve derivative reporter ( $-Pn^{-1}$ ); **B–F** expression of HMGR, MVD, FPPS, SS, SE enzyme genes in the G1 to G7 groups

### Correlation analysis between key enzyme gene expression and efficacy component content

The correlation between the expression of key enzyme genes and the contents of efficacy components of *A. orientale* reared under different light intensities was analyzed, and the results are shown in Table 2. The expression of key enzyme genes was significantly correlated with the contents of total triterpene and index components. The correlation coefficients between the expression of key enzyme genes MVD, SE, and HMGR were 0.906, 0.858, and 0.855. The correlation coefficient between total triterpene content and index components was high, and the correlation coefficient between total triterpene content and alisol C 23-acetate was

slightly higher than that between total triterpene content and alisol B 23-acetate. For the correlation between the expression of key enzyme genes and the contents of functional components, the correlation coefficients between the content of total triterpenoid components and the expression of HMGR, MVD, and SE enzyme genes were higher than those of the index components, and the correlation coefficients between the index components and the expression of the SS gene were highest, which were 0.847 and 0.830.

It should be noted that the correlation between the expression of key enzyme genes and the efficacy component contents of *A. orientale* were not consistent. As shown in Fig. 6A, the expression levels of key enzyme genes HMGR and MVD were negatively correlated with the contents of

**Table 2** Analysis of correlation between gene expression and active content of *A. orientale*

Factors	Expression of key enzyme genes and content of active ingredients							
	HMGR	MVD	FPPS	SS	SE	Total triterpene	Alisol B 23-acetate	Alisol C 23-acetate
HMGR	1.000	0.855**	0.599**	0.699**	0.858**	0.893**	0.696**	0.730**
MVD		1.000	0.594**	0.734**	0.906**	0.872**	0.658**	0.709**
FPPS			1.000	0.560**	0.671**	0.704**	0.677**	0.719**
SS				1.000	0.736**	0.832**	0.847**	0.830**
SE					1.000	0.835**	0.647**	0.664**
Total triterpene						1.000	0.889**	0.922**
Alisol B 23-acetate							1.000	0.929**
Alisol C 23-acetate								1.000

\*\*Indicates extremely significant correlation ( $p \leq 0.01$ )

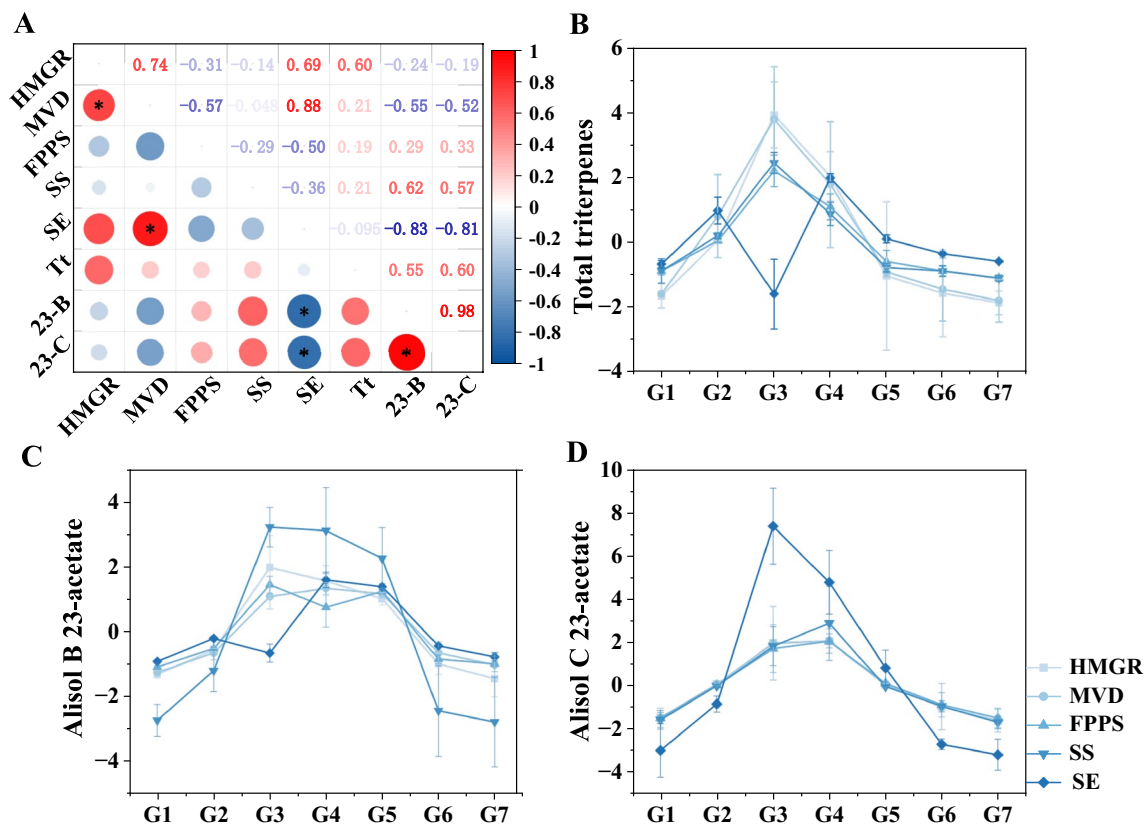


**Fig. 6** Correlation analysis between key enzyme genes and content of effective components in *A. orientale*. **A** Correlation heat map. **B** Estimated marginal means of Total triterpene. **C** Estimated marginal

means of Alisol B 23-acetate. **D** Estimated marginal means of Alisol C 23-acetate. *Tr* Total triterpenes; *23-B* alisol B 23-acetate; *23-C* alisol C 23-acetate. \*Indicates correlation ( $*p \leq 0.05$ )

the index components, but positively correlated with total triterpene content. Although the expression levels of key enzyme genes FPPS, SS, and SE were consistent with the content of functional components, their correlation between the content of index components was significantly higher than that for total triterpene content, and the negative correlation between the expression level of SS and the contents of index components was significantly different.

For groups G1 to G7, the standardized residuals of regression between the expression of key enzyme genes and the content of protostane triterpenes followed  $N(0, 1)$ , which is the standard normal distribution. The estimated boundary means of the standardized residuals for the three triterpenoid components are shown in Fig. 6B–D. The correlations between total triterpene, alisol B 23-acetate, alisol C 23-acetate, and the five key enzyme genes were all strongest for the G3–G5 groups. In particular, in the G3 treatment group, the correlations of SE with total triterpene and alisol B 23-acetate were significantly lower than for the other four key enzyme genes, as well as alisol C 23-acetate. These results indicate that the expression of the SE gene may be most closely related to the synthesis of alisol C 23-acetate under G3 light intensity.

## Discussion

As an energy source and signaling factor necessary for plant growth (Libatique et al. 2020), light plays an important role in plant physiological processes and primary metabolic activities. As an indicator of plant growth and development, dry weight can directly reflect the differences in primary metabolism among individuals. The active components are the products of secondary metabolism synthesis and accumulation of medicinal plants, and their contents reflect the degree and resistance of external stress to medicinal plants (Cheng et al. 2021). The expression of key enzyme genes can respond to changes in the external environment, regulating the synthesis and accumulation of secondary metabolites through differences in their expression (Wang et al. 2022). Based on these theories, we investigated the effects of light intensity on the contents of dry weight, protostane triterpenes and the expression of key enzymes for their biosynthesis in *A. orientale*.

Light intensity can affect the primary metabolic process of plants by affecting the photosynthetic rate and thus the accumulation of secondary metabolites (Roerber et al. 2021). Our results showed that increasing light intensity



promotes dry matter accumulation by *A. orientale* within a certain limit. In the range 50–400  $\mu\text{mol m}^{-2}\cdot\text{s}^{-1}$ , the dry weight of the whole plant, leaf, tubers and root of *A. orientale* increases with light intensity. However, when the light intensity exceeds 400  $\mu\text{mol m}^{-2}\cdot\text{s}^{-1}$ , the total dry weight and that of each part of the plant decrease. These results indicate that light intensity exceeding a certain limit damages the plant body, thereby affecting its growth and metabolic activities. According to the dry weight accumulation and changes after different light treatments, the suitable range of dry matter accumulation of *A. orientale* was 300–500  $\mu\text{mol m}^{-2}\cdot\text{s}^{-1}$ .

Secondary metabolites can also be effective medicinal substances and are produced by the interactions between genetic factors and environmental factors. The accumulation of secondary metabolites is regulated by the expression of gene in their biosynthetic pathways. Studies have shown that light intensity can affect the accumulation of active components in medicinal plants and the expression of genes for key enzymes in the biosynthetic pathways of active components (Appolloni et al. 2022; Cheng et al. 2021; Hernández et al. 2022; Pan and Guo 2016; Zhang et al. 2021; Wang et al. 2020b). In this study, the contents of total triterpenoids and index components and the expression of key enzyme genes increased first and then decreased with the increase of light intensity. When the light intensity was 200  $\mu\text{mol m}^{-2}\cdot\text{s}^{-1}$ , the total triterpene content in the tubers was significantly higher than those in the other groups, and the expression of genes for the key enzymes HMGR, MVD, and SE were high. The expression levels of HMGR, FPPS, MVD, SS, and SE were significantly correlated with total triterpene content and index component content, indicating that the biosynthesis of triterpene requires the participation and synergistic regulation of multiple key enzyme genes. Further correlation analysis showed that there was a significant positive correlation between the key enzyme gene MVD and HMGR, MVD and SE, and index components, indicating that there were positive regulatory effects within the key enzyme genes and index components. There was a significant negative correlation between the index component and SE gene, indicating that the key enzyme gene SE might be one of the rate-limiting enzymes for the synthesis of protostane triterpenes. The relationship between the expression of key enzyme genes and protostane triterpenes was analyzed under different light intensities. The correlation was the strongest under the light intensity range 200–400  $\mu\text{mol m}^{-2}\cdot\text{s}^{-1}$ . Notably, the correlation between SE enzyme gene expression and total triterterpene and Alisol B 23-acetate was lowest at 200  $\mu\text{mol m}^{-2}\cdot\text{s}^{-1}$ , and the correlation with Alisol C 23-acetate was significantly highest at this time, indicating that high SE expression at light intensity of 200  $\mu\text{mol m}^{-2}\cdot\text{s}^{-1}$  may promote massive synthesis of Alisol C 23-acetate. The correlations between expression of key

enzyme genes and protostane triterpenes were strongest in the light intensity range of 200–400  $\mu\text{mol m}^{-2}\cdot\text{s}^{-1}$ .

These results indicate that triterpene biosynthesis requires the participation and coordination of multiple key enzyme genes and that light intensity affects the accumulation of protostane triterpenes in *A. orientale* by regulating the expression of key enzymes in triterpenoid biosynthesis. The environment suitable for the growth and development of medicinal plants is different from the environment suitable for the accumulation of secondary metabolites (Huang et al. 2022). In this study, the dry matter accumulation of plants under the light intensity of 200  $\mu\text{mol m}^{-2}\cdot\text{s}^{-1}$  was slightly lower than that under the light intensity of 300  $\mu\text{mol m}^{-2}\cdot\text{s}^{-1}$ , but the total triterpene content was significantly higher and the index component content reached its maximum. The index component content for plants reared at 200  $\mu\text{mol m}^{-2}\cdot\text{s}^{-1}$  was slightly lower than that at 300  $\mu\text{mol m}^{-2}\cdot\text{s}^{-1}$ , but the dry matter accumulation was the highest. When the light intensity was 500  $\mu\text{mol m}^{-2}\cdot\text{s}^{-1}$ , although dry weight was at a high value, protostane triterpenes and expression of key enzyme genes were at a low value while the correlation was low. In conclusion, a light intensity in the range 200–400  $\mu\text{mol m}^{-2}\cdot\text{s}^{-1}$  is more conducive to the growth of *A. orientale* seedlings and the accumulation of protostane triterpenes.

In conclusion, light intensity regulates the accumulation of prototerpene-type triterpenoid components in *A. orientale* by regulating the expression of key enzyme genes involved in protostane triterpene biosynthesis. Appropriate light intensity can promote the accumulation of dry matter and the biosynthesis of effective substances in *A. orientale*. These results lay a foundation for elucidating the molecular mechanism by which light intensity regulates the accumulation of protostane triterpenes and provide practical guidelines for the scientific and rational production of *A. orientale*.

**Acknowledgements** The authors thank all the farmers of *Alisma orientale* in Jian'ou City, Fujian Province for providing seedlings and preserving excellent germplasm. We wish to thank the anonymous reviewers for valuable comments on the manuscript.

**Author contributions** All authors contributed to the study conception and design. WQ Wu and SM Li contributed equally to this work. W Gu and R Tian designed and revised the manuscript. M Luo and JJ Tang performed the experiments and collected data. WQ Wu and SM Li wrote the manuscript. M Tang and YZ Wu analyzed the data. All authors have read and approved the manuscript.

**Funding** This research was supported by the National Natural Science Foundation of China (Grant No. 82073958 and 81673534), research of assurance ability improvement of Chinese medicinal resources(2023). Data availability The data that support the findings of this study are available on request from the corresponding author.

**Data availability** The data that support the findings of this study are available from the corresponding author (Wei Gu) upon reasonable request.

## References

- Appolloni E, Pennisi G, Zauli I, Carotti L, Paucek I, Quaini S, Orsini F, Gianquinto G (2022) Beyond vegetables: effects of indoor LED light on specialized metabolite biosynthesis in medicinal and aromatic plants, edible flowers, and microgreens. *J Sci Food Agric* 102:472–487
- Cheng XY, Ouyang JM (2023) Carboxymethylated rhizoma alismatis polysaccharides regulate calcium oxalate crystals growth and reduce the regulated crystals' cytotoxicity. *Biomolecules* 13:1044
- Cheng Y, Liu H, Tong X, Liu Z, Zhang X, Chen Y, Wu F, Jiang X, Yu X (2021) Effects of shading on triterpene saponin accumulation and related gene expression of *Aralia elata* (Miq.) Seem. *Plant Physiol Biochem* 160:166–174
- Choi E, Jang E, Lee JH (2019) Pharmacological activities of *Alisma orientale* against nonalcoholic fatty liver disease and metabolic syndrome: literature review. *Evid Based Compl Alternat Med* 2019:2943162
- Dou F, Miao H, Wang JW, Chen L, Wang M, Chen H, Wen AD, Zhao YY (2018) An Integrated lipidomics and phenotype study reveals protective effect and biochemical mechanism of traditionally used *Alisma orientale* Juzepzuk in chronic kidney disease. *Front Pharmacol* 9:53
- Fan J, Jiang H, Sun L, Zhang Q, Liu H (2021) Effect of rhizoma alismatis on the expression of hub genes in the treatment of gastric cancer. *Transl Cancer Res* 10:4087–4095
- Feng L, Liu TT, Huo XK, Tian XG, Wang C, Lv X, Ning J, Zhao WY, Zhang BJ, Sun CP, Ma XC (2021) *Alisma* genus: phytochemical constituents, biosynthesis, and biological activities. *Phytother Res* 35:1872–1886
- Gao X, Sun C, Yu Z, Cang J, Tian X, Huo X, Feng L, Liu X, Wang C, Zhang B, Ma X (2018) Correlation analysis between the chemical contents and bioactivity for the quality control of alismatis rhizoma. *Acta Pharm Sin B* 8:242–251
- Hernández KV, Moreno-Romero J, Hernández de la Torre M, Manríquez CP, Leal DR, Martínez-García JF (2022) Effect of light intensity on steviol glycosides production in leaves of *Stevia rebaudiana* plants. *Phytochemistry* 194:113027
- Huang Y, Zhai Y, Huang Y, Huang Y, Liu K, Zhang J, Zhou J (2022) Effects of light intensity on physiological characteristics and expression of genes in coumarin biosynthetic pathway of *Angelica dahurica*. *Int J Mol Sci* 23(24):15912
- Hwang YH, Kang KY, Lee SJ, Nam SJ, Son YJ, Yee ST (2016) The protective effects of alisol A 24-acetate from *Alisma canaliculatum* on ovariectomy induced bone loss in vivo. *Molecules* 21:74
- Jang E, Lee JH (2021) Promising anticancer activities of alismatis rhizome and its triterpenes via p38 and PI3K/Akt/mTOR signaling pathways. *Nutrients* 13(7):2455
- Ji YY, Gu W, Qiu RL, Tian R, Wei CB, Li T, Zhu Y, Lang PL (2023) Effects of light intensity on growth and physio-biochemical characteristics of *Alisma orientale* (Sam.) Juzep. *Mol Plant Breed* 1–14
- Kuo CH, Chou YC, Liao KC, Shieh CJ, Deng TS (2020) Optimization of light intensity, temperature, and nutrients to enhance the bioactive content of hyperforin and rutin in *St John's Wort*. *Molecules* 25(18):4256
- Li Y, Kong D, Fu Y, Sussman MR, Wu H (2020) The effect of developmental and environmental factors on secondary metabolites in medicinal plants. *Plant Physiol Biochem* 148:80–89
- Libatique MJH, Lee MC, Yeh HY (2020) Effect of light intensity on the mechanism of inorganic arsenic accumulation and patterns in the red macroalga, *sarcodia suaia*. *Biol Trace Elem Res* 195:291–300
- Luan ZL, Ming WH, Sun XW, Zhang C, Zhou Y, Zheng F, Yang YL, Guan YF, Zhang XY (2021) A naturally occurring FXR agonist, alisol B 23-acetate, protects against renal ischemia-reperfusion injury. *Am J Physiol Renal Physiol* 321:F617–f628
- Pan J, Guo B (2016) Effects of light intensity on the growth, photosynthetic characteristics, and flavonoid content of *epimedium pseudowushanense* B. L. Guo. *Molecules* 21(11):1475
- Roeber VM, Bajaj I, Rohde M, Schmülling T, Cortleven A (2021) Light acts as a stressor and influences abiotic and biotic stress responses in plants. *Plant Cell Environ* 44:645–664
- Shen J, Wei W, Wang X, Yang J, Lu L, Lv X, Xue X (2020) Proliferation of vascular smooth muscle cells under ox-LDL is regulated by alismatis rhizoma decoction via Inhibiting ERK1/2 and miR-17~92a cluster activation. *Evid Based Compl Alternat Med* 2020:7275246
- Shu Z, Pu J, Chen L, Zhang Y, Rahman K, Qin L, Zheng C (2016) *Alisma orientale*: ethnopharmacology, phytochemistry and pharmacology of an important traditional Chinese medicine. *Am J Chin Med* 44:227–251
- Wang P, Song T, Shi R, He M, Wang R, Lv J, Jiang M (2020a) Triterpenoids from *Alisma* species: phytochemistry, structure modification, and bioactivities. *Front Chem* 8:363
- Wang Z, Xiao S, Wang Y, Liu J, Ma H, Wang Y, Tian Y, Hou W (2020b) Effects of light irradiation on essential oil biosynthesis in the medicinal plant *Asarum heterotropoides* Fr. Schmidt var. *mandshuricum* (Maxim) Kitag. *PLoS ONE* 15:e0237952
- Wang D, Yang T, Li Y, Deng F, Dong S, Li W, He Y, Zhang J, Zou L (2022) Light intensity—a key factor affecting flavonoid content and expression of key enzyme genes of flavonoid synthesis in tartary buckwheat. *Plants (basel)* 11(16):2165
- Wu Y, Wang X, Yang L, Kang S, Yan G, Han Y, Fang H, Sun H (2023) Therapeutic effects of *Alisma orientale* and its active constituents on cardiovascular disease and obesity. *Am J Chin Med* 51:623–650
- Xu X, Li L, Zhang Y, Lu X, Lin W, Wu S, Qin X, Xu R, Lin W (2020) Hypolipidemic effect of *Alisma orientale* (Sam.) Juzep on gut microecology and liver transcriptome in diabetic rats. *PLoS ONE* 15:e0240616
- Yan P, Wei Y, Wang M, Tao J, Ouyang H, Du Z, Li S, Jiang H (2022) Network pharmacology combined with metabolomics and lipidomics to reveal the hypolipidemic mechanism of *Alismatis rhizoma* in hyperlipidemic mice. *Food Funct* 13:4714–4733
- Yao L, Lu J, Wang J, Gao WY (2020) Advances in biosynthesis of triterpenoid saponins in medicinal plants. *Chin J Nat Med* 18:417–424
- Zhang LL, Xu W, Xu YL, Chen X, Huang M, Lu JJ (2017a) Therapeutic potential of rhizoma alismatis: a review on ethnomedicinal application, phytochemistry, pharmacology, and toxicology. *Ann NY Acad Sci* 1401:90–101
- Zhang X, Li XY, Lin N, Zhao WL, Huang XQ, Chen Y, Huang MQ, Xu W, Wu SS (2017b) Diuretic activity of compatible triterpene components of alismatis rhizoma. *Molecules* 22:1459
- Zhang S, Zhang L, Zou H, Qiu L, Zheng Y, Yang D, Wang Y (2021) Effects of light on secondary metabolite biosynthesis in medicinal plants. *Front Plant Sci* 12:781236
- Zheng BQ, Zou LH, Li K, Wan X, Wang Y (2017) Photosynthetic, morphological, and reproductive variations in *Cypripedium tibeticum* in relation to different light regimes in a subalpine forest. *PLoS ONE* 12:e0181274
- Zhou X, Luo J, Lin S, Wang Y, Yan Z, Ren Q, Liu X, Li X (2023) Efficacy of *poria cocos* and alismatis rhizoma against diet-induced hyperlipidemia in rats based on transcriptome sequencing analysis. *Sci Rep* 13:17493
- Zhu HC, Jia XK, Fan Y, Xu SH, Li XY, Huang MQ, Lan ML, Xu W, Wu SS (2021) Alisol B 23-acetate ameliorates azoxymethane/dextran sodium sulfate-induced male murine colitis-associated colorectal cancer via modulating the composition of gut

microbiota and improving intestinal barrier. *Front Cell Infect Microbiol* 11:640225

**Publisher's Note** Springer Nature remains neutral with regard to jurisdictional claims in published maps and institutional affiliations.

Springer Nature or its licensor (e.g. a society or other partner) holds exclusive rights to this article under a publishing agreement with the author(s) or other rightsholder(s); author self-archiving of the accepted manuscript version of this article is solely governed by the terms of such publishing agreement and applicable law.